Department of Biotherapy[1], Cancer Center, West China Hospital, Sichuan University, Chengdu; Changzhou Yinsheng Pharmaceutical Company[2], Changzhou; School of Life Science and Engineering[3], Southwest JiaoTong University, Chengdu, China

A novel fixed-dose combination treatment for chronic hepatitis C, based on NS5A inhibitor fopitasvir and NS5B inhibitor sofosbuvir

Shu-yan Zhou[1,#], Xin-yi Chen[1,#], Yan Chen[1], Na-na Meng[1], Xin Tao[2], Hua-long He[1], Zhi-hao Liu[1], Ning-yu Wang[3,*], Luo-ting Yu[1,*]

Received December 18, 2020, accepted March 20, 2021

**Corresponding authors: Luo-ting Yu, Department of Biotherapy, Cancer Center, West China Hospital, Sichuan University, Chengdu*
yuluot@scu.edu.cn
Ningyu Wang, School of Life Science and Engineering[3], Southwest JiaoTong University, Chengdu, China
wangny-swjtu@swjtu.edu.cn
[#]These authors contributed equally to this work.

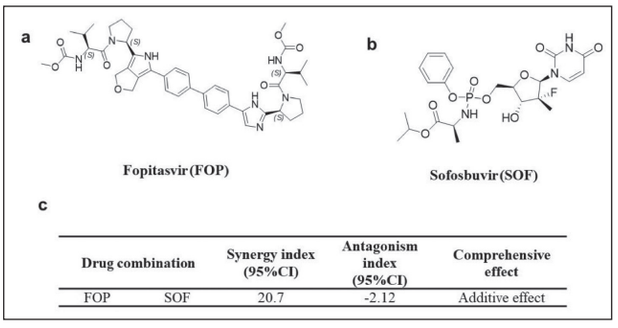
Pharmazie 76: 372-378 (2021) *doi: 10.1691/ph.2021.0190*

Drug resistance caused by the extreme genetic variability of zhe hepatitis C virus has rendered effective combinations of drugs indispensable in the treatment of chronic hepatitis C (CHC). Herein, we developed a fixed-dose combination (FDC) treatment containing the NS5B inhibitor sofosbuvir (SOF) and the NS5A inhibitor fopitasvir (FOP). Then the dissolution behavior of FOP in FOP/SOF FDC was improved by co-micronizing FOP with lactose. The enhanced dissolution rate of FOP in the FDC was in good agreement with the behavior of the FOP single-drug tablet. In addition, pharmacokinetic studies showed that both FOP and SOF in the FDC exhibited similar characteristics (area under the curve, C_{max}, T_{max}, and $T_{1/2}$) as those of tablets containing FOP or SOF alone. These results revealed that the FOP/SOF FDC represents a potential therapeutic option for the treatment of CHC.

1. Introduction

Chronic hepatitis C (CHC) represents an infectious disease caused by the pathogen hepatitis C virus (HCV) (Heffernan et al. 2019). Although the direct-acting antiviral agents (DAAs) have achieved high sustained virologic response (SVR) rates in CHC patients, cirrhosis and other chronic diseases caused by CHC still led to an estimated 399,000 death worldwide in 2016 (WHO 2017) and the efficacy of DAAs is still limited by the mutations caused by rapid replication rate of HCV and low fidelity of RdRp (Li and De Clercq 2017; Sandmann et al. 2019; Villani et al. 2019). Thus, rapid development of drug-resistant strains is demanding urgent search for more effective therapeutic options (Marks and Naggie 2019; Sagnelli et al. 2018; Sandmann et al. 2019; Torre et al. 2016). Fopitasvir (FOP; Fig. 1a), a novel HCV NS5A inhibitor developed in our laboratory, is potently active against HCV genotypes 1-6 (Tao et al. 2019). FOP showed good safety and effectiveness when combined with other DAAs proved by Phase I and II clinical trials (NMPA CDE, 2021). However, long-term use of any DAA alone increases the risk of drug resistance (Dietz et al. 2018). Sofosbuvir (SOF; Fig. 1b) is a nucleotide analog prodrug that inhibits different genotypes of HCV by competitively antagonizing NS5B (Aunins et al. 2018; Lam et al. 2012; Murakami et al. 2010; Sofia et al. 2010). Furthermore, it has a higher resistance barrier (Halfon and Sarrazin 2012; McCown et al. 2008). At present, several combination drug regimens and fixed-dose combinations (FDCs) have shown good therapeutic effects, such as Harvoni (SOF/daclatasvir) (Araujo et al. 2019; Ascher et al. 2014) and Epclusa (SOF/velpatasvir) (Heo and Deeks, 2018; von Felden et al. 2018). In a previous study FOP and SOF have an additive effect on drug resistance *in vitro* (Fig. 1c). Therefore, the combination of FOP and SOF is expected to produce good therapeutic effects in hepatitis C patients.

Patient compliance is critical to successful treatment of chronic conditions (Bangalore et al. 2007), and the inverse correlation between the complexity of a drug regimen and medication adherence is well established (Pan et al. 2008). FDCs decrease the risk of medication non-compliance, which can translate into better clinical outcomes. (Cazzola and Matera, 2017). Accordingly, development of FOP/SOF FDCs may contribute to the treatment of CHC. Herein, we report the development of FOP/SOF FDCs and the method of improving the solubility and dissolution rate of FOP in FOP/SOF FDC.



c

Drug combination		Synergy index (95%CI)	Antagonism index (95%CI)	Comprehensive effect
FOP	SOF	20.7	-2.12	Additive effect

Fig. 1: Chemical structures of FOP (a) and SOF (b). (c) Combination effect index of FOP and SOF in GT1b replicon cell experiment (Unit: μM2%). The Combination effect index description: positive index represents a synergistic effect and a negative index represents an antagonistic effect; Absolute value of the index that is <25 indicates additive effect. The experimental data were processed using MacSynegy software for the analysis of the effects of FOP combined with SOF.

2. Investigations and results

2.1. Chemical compatibility studies between FOP, SOF and excipients

Chemical compatibility studies were performed for FOP and SOF in the presence of various excipients, selected from existing excipients of FOP tablets and SOF tablets (EMC, 2021), in order to evaluate any instability (incompatibility) amongst drugs and excipients.

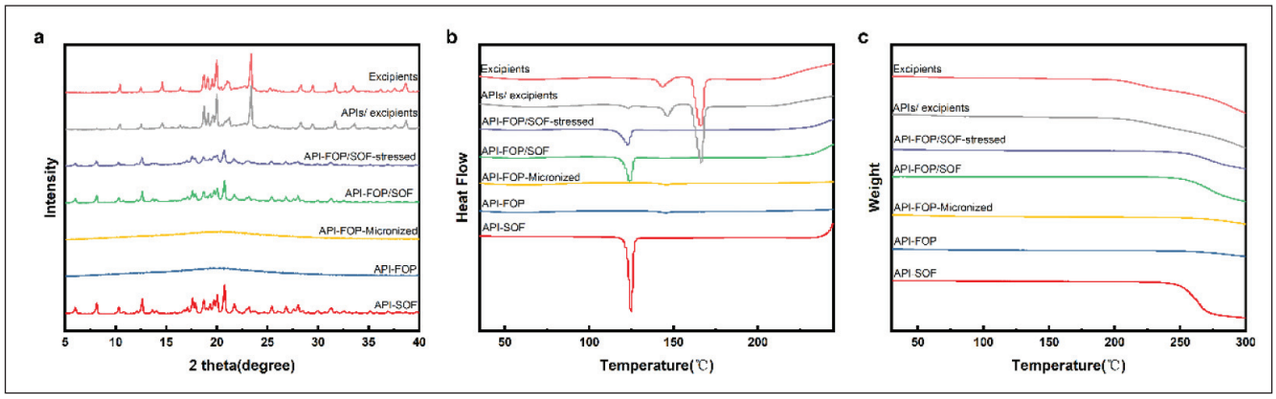


Fig. 2: Crystal form of compatibility samples (day 0). (a) X-ray powder diffraction (XRD). (b) Differential scanning calorimetry (DSC). (c) Thermal gravimetric analysis (TGA).

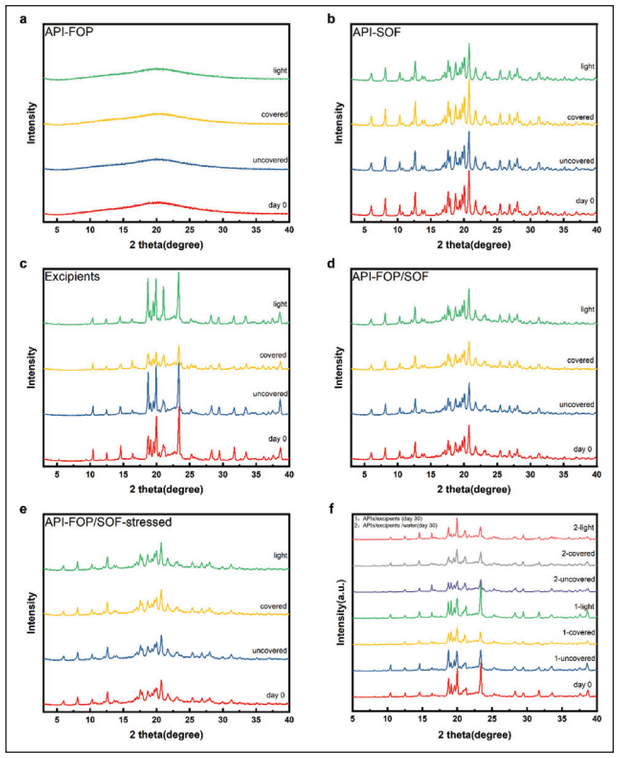


Fig. 3: XRD patterns in the research of drug-excipient compatibility under stressed conditions (day 0 and day 30). Among them, covered refers to the condition:40 °C ± 2 °C / 75% relative humidity (RH) ± 5% RH, sealed with rubber plug; Uncovered refers to the condition: 40 °C ± 2 °C/75% RH ± 5% RH; light: 4500lux intensity.

2.2.1. *Investigation of crystal forms*

X-ray powder diffraction (XRD) is a powerful technique used for discriminating the physical state of components of solid phases (Leuner and Dressman 2000). As shown in Fig. 2, SOF is in the crystalline state, which showed intense characteristic diffraction peaks. There are strong diffraction peaks in the curve of the mixed excipients. Two broad diffusion amorphous halos were observed in the XRD patterns of API-FOP and API-FOP-micronized, which revealed their amorphous state.

Besides, differential scanning calorimetry (DSC) can check the crystal morphology by quantitatively detecting the energy change of the samples. From Fig. 2b, the crystalline SOF only displayed an endothermic melting peak at 125 °C, and mixture of excipients showed melting points at about 145°C and 160°C. No melting peak was detected from the DSC curves of API-FOP and API-FOP-micronized. This finding further confirmed the amorphous structure of API-FOP and API-FOP-micronized obtained by XRD. After the operations of micronizing (API-FOP-micronized), mixing (API-FOP/SOF, APIs/excipients) and pressing (API-FOP/SOF-stressed), the characteristic peaks of XRD and DSC of FOP and SOF are basically the same as those of the original samples (Fig. 2a-2c). In addition, as shown in Fig. 2a, some diffraction peaks of SOF disappeared after mixing with excipients because a large number of excipients masked the diffraction phenomenon of SOF crystal. The melting peak of SOF (at 125 °C) in the curve of APIs/excipients can also prove this point.

Samples were stored under accelerated conditions for 30 days to predict the compatibility. Diffraction patterns of the samples at day 30 were similar to the curves in initial, no matter under which conditions (Fig. 3). These results demonstrated that the conditions we have simulated (high temperature, high humidity, light, oxygen, and other conditions during preparation, which may influence the quality of the tablets) had little effect upon the crystal transformation of SOF and FOP, regardless of the presence of excipients.

2.2.2. *Determination of related substances*

In the investigation of related substances (Table 1), the content of the largest single impurity, the number of impurities and the total impurity content in the FOP samples under the light condition rose extremely fast, while FOP is relatively stable under other conditions. The impurity of SOF enhanced slightly under all conditions. In the group of API-FOP/SOF, there was a minor impurity change compared with the sum of impurities in the individual SOF and FOP groups. The impurities in API-FOP/SOF-stressed groups were significantly reduced compared with the API-FOP/SOF groups. Besides, the impurity content of the API/excipient groups was less than that of the API-FOP/SOF groups, too. These trends of related substances indicated that the stability of FOP may benefit from pressing and mixing due to the reduction of the exposed area. The addition of 5% water (API/excipient/water) slightly increased the total impurity content, suggesting the storage time of materials after granulation and assay of water in tablets should be controlled. Overall, there was a relatively good compatibility between FOP, SOF and the excipients used in this study. Instability of FOP under light conditions could be increased by reducing of the illuminated area. Hence FOP/SOF FDC tablets can be coated and packaged to solve the stability problem.

2.2. *The low dissolution of FOP in FOP/SOF FDC tablets*

After studying the chemical compatibility of drug and excipients, FOP/SOF FDC tablets were prepared as shown in Table 2. Then the FDC were tested according to ChP to evaluate the feasibility of the formulation process (Bhalerao et al. 2020; Jantratid et al. 2008). The dissolution of FOP/SOF FDC was examined (Fig. 4). The dissolution rate and the final cumulative dissolution of FOP (FOP-S1) in the FOP/SOF FDC were significantly lower than the level of FOP tablets (FOP-R1). We assume that the low solubility

Table 1: Determination of related substances

Samples	Conditions	Day 0	Day 15			Day 30		
			Covered	Uncovered	Light	Covered	Uncovered	Light
API-FOP	SLI	0.13	0.19	0.18	2.08	0.24	0.26	2.09
	Count	13	19	17	46	16	17	55
	Total	0.66	1.54	1.42	10.57	1.16	1.30	10.65
API-SOF	SLI	0.13	0.37	0.35	0.33	0.16	0.15	0.18
	Count	4	9	9	9	6	5	5
	Total	0.40	1.82	1.42	1.07	0.52	0.47	0.52
API-FOP/SOF	SLI	0.25	0.34	0.35	2.25	0.49	0.50	3.12
	Count	11	17	19	37	15	15	45
	Total	1.29	3.06	2.84	10.70	2.59	2.34	12.75
API-FOP/SOF-stressed	SLI	0.60	0.16	0.17	0.60	0.24	0.27	0.81
	Count	26	19	15	26	15	15	27
	Total	2.93	1.49	1.23	2.93	1.18	1.20	2.94
APIs/excipients	SLI	0.37	0.28	0.33	1.01	0.47	0.40	1.38
	Count	8	19	23	36	15	23	46
	Total	1.51	2.38	2.65	5.18	2.52	2.84	6.52
APIs/excipients/water	SLI	0.37	0.40	0.32	1.22	0.41	0.65	1.54
	Count	8	19	21	35	21	23	50
	Total	1.51	2.74	2.37	5.48	3.15	3.68	7.31

SLI: single largest impurity; Count: count of impurities; Total: Total impurities. Covered refers to the condition of 40 °C ± 2 °C/75% relative humidity (RH) ± 5% RH, sealed with rubber plug; Uncovered refers to the condition of 40 °C ± 2 °C/75% RH ± 5% RH; 4500 LUX refers to under light conditions with 4500lux intensity.

Table 2: Composition of FOP/SOF FDC

	Materials	Single dose/mg	Proportion/%
Core	SOF	400	60.88
	FOP	60	9.13
	Lactose	100	15.22
	Cross-linked carboxymethyl cellulose sodium	26	3.96
	Polyvidone	20	3.04
	Purified water*	380	/
	Microcrystalline cellulose	44	6.70
	Magnesium stearate	7	1.07
Coating layer	Film coating premix	32.85	/
	Purified water*	241.9	/
Weight	/	689.85	/

*The purified water was removed by drying.

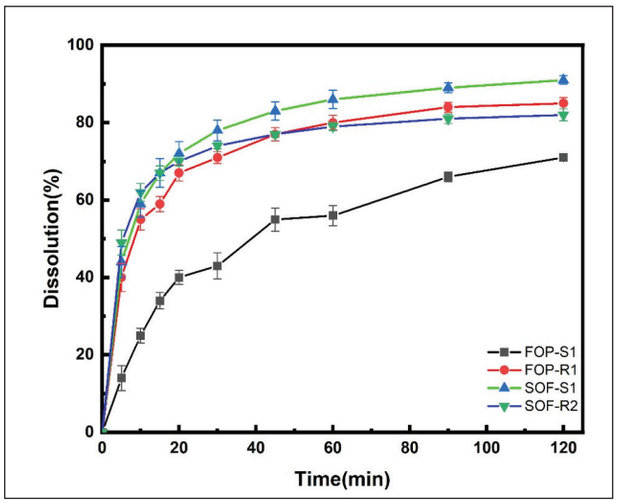


Fig. 4: Dissolution behaviors of FOP or SOF in FOP/SOF FDC (S1) and single agents (R1: FOP tablets; R2: SOF tablets). (n=6)

of FOP might be the most critical point for its absorption *in vivo*, and the poor dissolution behavior of FOP in FOP/SOF FDC may affect its bioavailability, so increasing the dissolution rate of FOP in FOP/SOF FDC is urgent for this study.

2.3. Increasing the dissolution of FOP in FOP /SOF FDC tablets

FOP is a strongly hydrophobic, insoluble drug and presents in stable amorphous form state. The dissolution rate and solubility of FOP can be improved by increasing the specific surface area and hydrophilicity in the light of Noyes-Whitney equation. Hence, some pretreatment methods of FOP had been studied such as micronizing, co-milling FOP with lactose in different ratio (m/m: 1/1 or 1/2) and size. Different powders were prepared and analyzed. First, the FOP and lactose FOP physical mixing group (FOP/Lac) were set as references to investigate the changes in the solubility of the different powders. It can be observed from Fig. 5a that lactose had little direct effect on promoting the dissolution behavior of FOP (green). The dissolution rate of FOP was significantly improved by micronizing and co-micronizing FOP with lactose independent of the mass ratio (1:1, 1:2) and size (the particle size of a sample when the cumulative particle size distribution reaches 90% [D90]): 24 μm, 12 μm). However, these methods hardly raised the solubility of FOP.

The contact angles of different powders were analyzed to characterize powders' hydrophilicities (Fig. 5b). Co-micronizing significantly reduced the contact angle of powders, but micronizing FOP alone had no such effect. The contact angle of Co-micronized powder 3 decreased more, compared to contact angles of Co-micronized powder 1 and Co-micronized powder 2. These data suggested that hydrophilicity increased with the decreasing of powder's particle size in the presence of lactose.

Using pretreated FOP, The FOP/SOF FDCs tablets were prepared according to Table 2 and with the same procedures as before. The dissolutions of FOP in FOP/SOF FDCs *in vitro* were focused on. From Fig. 5c, the dissolution rate and solubilities of FOP in FOP/SOF FDCs containing Co-micronized powders were improved to varying degrees. Most importantly, the dissolution behavior of FOP has been greatly improved in the FOP/SOF FDC prepared by co-micronized powders 3, which is similar to the dissolution behavior of FOP tablets.

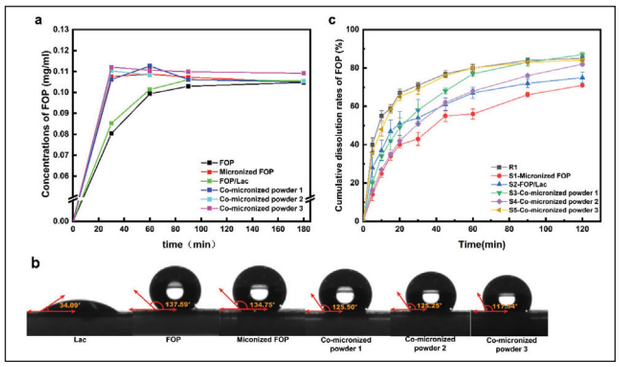


Fig. 5: (a) Solubility curves of FOP treated by different methods. FOP: untreated FOP; Micronized FOP: powder of FOP after micronizing; FOP/Lac: Physical mixture of FOP and lactose 1:1 (m/m); Co-micronized powder 1: co-micronized composite powder [FOP: lactose = 1:1 (m/m)], D90 = 24μm; Co-micronized powder 2: co-micronized composite powder [FOP: lactose = 1:2 (m/m)]; Co-micronized powder 3: Composite powder was micronized twice, FOP and lactose in 1:1 (m/m), D90=12μm. (b) The contact angle of water droplets on the surface of the powders at 293K. (c) The cumulative dissolution rates of FOP in FDCs (S) and FOP tablets (R), N=6. Treatments of FOP in different FDCs were marked on the picture. R1: FOP tablets; S1: FOP is micronized; S2: premixed with FOP and lactose; S3: FOP and lactose were co-micronized in 1:1 (m/m), D90 = 24 μm; S4: FOP and lactose were co-micronized in 1:2 (m/m); S5: FOP and lactose were co-micronized twice in 1:1 (m/m), D90 = 12 μm.

To further study the possible reasons for the pretreated technology of FOP improving the dissolution behavior of FOP in the FOP/SOF FDCs tablets, composite powders were analyzed by scanning electron microscopy (SEM). As shown in Fig. 6, the FOP particles had sharp edges, while the edges of lactose particles were soft. SEM images illustrated that lactose particles were adhered to the surface of FOP. The most important thing is that compared with the FOP/Lac image, the number of lactose particles attached was increased after co-micronization technology. At the same time, compared with micronizing FOP only, the static electricity of the co-micronization process was reduced, thereby greatly improving the output. We believe that the co-micronization technology promoted the electrostatic adsorption of lactose particles by FOP. The increasing amount of the attached lactose particles enhanced the hydrophilicity of the composite powder, which led to the improvement of the dissolution rate of FOP (Iqbal et al. 2011; Dong et al. 2018; Friedrich et al. 2006).

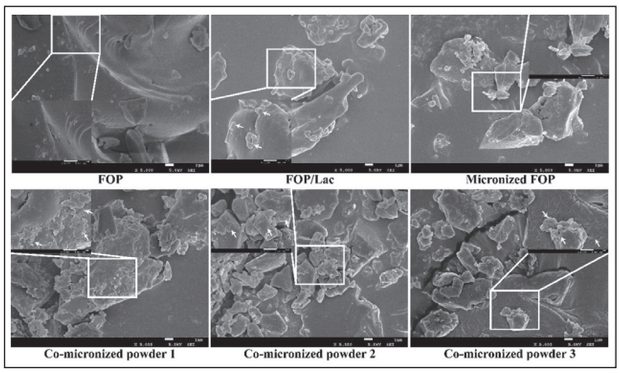


Fig. 6: Microstructure of powders after pretreating by different methods. Arrows: The position of the lactose particles.

2.4. *Pharmacokinetic evaluations of preparation*

The pharmacokinetic profiles of FOP tablets, SOF tablets and FOP/SOF FDC were determined in Sprague Dawley rats. Little discrepancy existed in the systemic exposure of FOP, including $AUC_{0\text{-last}}$ and C_{max}, within the FOP tablets and FOP/SOF FDC. The half-life and T_{max} of FOP in the FOP tablets and FOP/SOF FDCs were basically the same (Table 3 and Fig. 7 a). Previous studies demonstrated that little SOF is observed in rat plasma following oral administration because of high hydrolysis activity of phosphoramidates prodrugs in rodent plasma (Lam et al. 2010; Wang et al. 2020). Thus PSI-6206, a metabolite of SOF in plasma, was selected to investigate the pharmacokinetic profiles. Little distinctions were found in the systemic exposure of PSI-6206 between the SOF tablets and FOP/SOF FDC, including $AUC_{0\text{-last}}$ and C_{max}. The half-life and T_{max} of the PSI-6206 in SOF tablets and FOP/SOF FDC were comparable (Table 3 and Fig.7 b). These data showed that the pharmacokinetic behaviors of FOP and SOF in FOP/SOF FDC were consistent with those of FOP tablets and SOF tablets, respectively, which provided the basis for follow-up study.

Table 3: Pharmacokinetic parameters in rats after oral administration (mean ± SD, n = 3)

Group	Compound	$T_{1/2}$ (h)	T_{max} (h)	C_{max} (ng/mL)	$AUC_{(0\text{-}t)}$ (h*ng/mL)
FDC	PSI-6206	3.17 ± 0.59	2.65 ± 0.58	1012.94 ± 23.91	6140.78 ± 386.40
	FOP	1.74 ± 0.27	3.67 ± 0.58	1299.44 ± 100.16	5960.45 ± 528.70
SOF tablets	PSI-6206	3.24 ± 0.09	3.33 ± 0.58	972.84 ± 168.22	5361.71 ± 557.83
FOP tablets	FOP	1.93 ± 0.13	4.00 ± 0.00	974.58 ± 591.47	5808.59 ± 3969.50

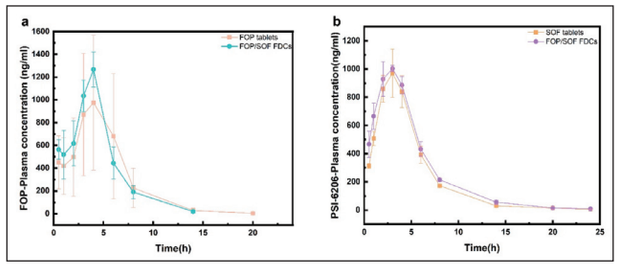


Fig. 7: Mean plasma concentration-time curves of FOP (a) and PSI-6216 (b) in rats after oral administration of FOP/SOF FDC, FOP tablets and SOF tablets at a dose of 5.4 mg/kg FOP and (or) 36 mg/kg SOF (mean ± SD, n = 3).

2.5. *Discussion and conclusion*

The combination of FOP and SOF is a potential treatment strategy for the treatment of CHC. In this study, we compared the crystal forms and the related substances of samples stored under different conditions, showing the good chemical stabilities between FOP, SOF and excipients. Then FOP/SOF FDC were prepared using selected excipients, while FOP in the FOP/SOF FDC did not show a good dissolution behavior *in vitro* due to the its low solubility. Therefore, we considered pretreatment methods of FOP such as micronization and co-micronization with lactose in different ratios and sizes. Experiments showed that these pretreatment methods can significantly improve the dissolution behavior of FOP in FOP/SOF FDC. Further analysis instated that the change in hydrophilicity of FOP, which may be caused by electrostatic adsorption, is the reason for improving the dissolution behavior of FOP in FOP/SOF FDCs. After using the pretreated FOP, the pharmacokinetic properties of FOP and SOF in the FOP/SOF FDC were almost the same as those in the single prescriptions.

Our study showed that co-micronizing insoluble drugs with lactose can enhance the solubility or reduce the electrostatic incorporation of materials. Therefore, lactose could be replaced by other hydrophilic materials and amphiphilic agents such as microcrystalline cellulose and sodium dodecyl sulfate. Perhaps the cost-effective co-micronization is worth being applied in the process of formulation development and production sometimes.

Compared with the pharmacokinetics of single prescriptions, profiles of FOP and SOF in the FOP/SOF FDC showed non-inferiority. The similarity of the pharmacokinetic characteristics ($AUC_{0\text{-last}}$, C_{max}, $T_{1/2}$, T_{max}) between FOP/SOF FDC and single prescriptions probably mean that FOP and SOF seem unlikely to interfere with each other *in vivo* (Bellesini et al. 2020). This result partly indicates there is little risk of drug interaction between FOP and SOF, and the FOP/SOF FDCs may have the same safety as single prescriptions. Based on the reported formulation and technology, abundant samples have been prepared for the stability study, and safety evaluation will be conducted after obtaining the pilot samples. In general, our research provides a solid foundation for the development of FOP/SOF FDC.

3. Experimental

3.1. Chemicals and reagents

FOP (active pharmaceutical ingredient [API]) was purchased from Changzhou Yinsheng Pharmaceutical Company (Changzhou, Jiangsu Province, China). The FOP reference (lot number: 201402-04-181101, mass fraction = 98.86%) and FOP tablets (batch: 20181203, containing FOP 30 mg) were donated by Changzhou Yinsheng Pharmaceutical Company. SOF (API) was purchased from Jiangsu Yong'an Pharmaceutical Co., Ltd. (Huai'an, Jiangsu Province, China). SOF tablets (Sovaldia®; batch: 17SB001D, containing SOF 400 mg) were purchased from Gilead Sciences Ireland UC. The SOF reference was purified and calibrated in the laboratory. The excipients (lactose, microcrystalline cellulose, cross-linked carboxymethylcellulose sodium, povidone, magnesium stearate, and gastric-soluble film coating premix) used in this work were of pharmaceutical grade and purchased from Yuandong Biopharmaceutical Co., Ltd. (Chengdu, Sichuan Province, China). All other chemicals and reagents used were of UPLC grade.

3.2. Drug-excipient compatibility studies

3.2.1. Preparation of samples

Excipients chosen were checked for their usage among the ones already used in commercial formulations with FOP and SOF. SOF (API-SOF), FOP (API-FOP), and excipients (lactose, microcrystalline cellulose, cross-linked carboxymethyl cellulose sodium, povidone, magnesium stearate and stomach-soluble film coating premix, mixed 20:20:20:5:5:20 [m/m]) were prepared as the control. FOP was micronized (API-FOP-micronized). The physical mixing of FOP and SOF was conducted at a ratio of 1:1 (m/m) (API-FOP/SOF), and the homogeneity of mixed powder was tested (relative standard deviation ≤5.0%, n = 6). API-FOP/SOF was pressed into pieces (average weight 60 mg; API-FOP/SOF-stressed). FOP, SOF, and blank excipients were mixed as APIs/excipients (1:1:90 [m/m]). Purified water was added into the composite powder of APIs/excipients at 0.5% (m/m; APIs/excipients/water). Each sample was divided into seven parts: T_0, 40±2 °C/75% relative humidity (RH) ± 5% RH; 40±2 °C/75% RH ± 5% RH, sealed; light conditions (4500 LUX). Samples were taken up till 1 month. Changes in the related substances of samples were detected at days 0, 15, and 30 using UPLC methods as described. Crystal form was only detected [X-ray powder diffraction (XRD); Differential scanning calorimetry (DSC)] at days 0 and 30.

3.2.3. Investigation of crystal forms

3.2.3.1. X-ray powder diffraction (XRD)

XPD was performed using a DX-2700B (DX-2700B, Dandong Haoyuan Instrument Co., Ltd., China) with a Cu-source and θ-2θ diffractometer equipped with a Lynx-eye Position Sensitive Detector. The generator was subjected to a voltage of 40 kV and a current of 30 mA. Samples were dispersed on a low background Si sample holder and compacted gently with the back of a metal spatula. Scans ran from 3° to 40° 2θ (data shown between 5° and 40° 2θ) with a 0.02 step size at 3 seconds per step.

3.2.3.2. Differential scanning calorimetry (DSC)

Thermograms of samples were recorded using a DSC 1 differential scanning calorimeter (Mettler Toledo DSC 1, Mettler-Toledo, Greifensee, Switzerland). Samples, 3-5 mg, were accurately weighed in 50 µL aluminum pans with pierced lids. The heating rate was 10 K/min, and the DSC scans were recorded between 35 °C and 250 °C; the flow rate of N_2 was 20 mL/min. (Wang et al. 2019).

3.2.3.3. Thermal gravimetric analysis (TGA)

Thermogravimetry of samples were recorded using a TGA 2 thermogravimetric analyzer (Mettler Toledo TGA 2, Mettler-Toledo, Greifensee, Switzerland). Approximately 5 mg of each sample were placed in a crucible with air as the reference. The flow rate of N_2 was 20 mL/min. The temperature was 35-350 °C, and the temperature rate was 10 K/min.

3.2.4. Determination of related substances

An appropriate amount of fine powder was collected and accurately weighed (about 30 mg SOF or 30 mg FOP). It was placed into a 50 mL volumetric flask, with diluent 1 (containing methanol and 0.01 M ammonium acetate buffer [pH4.0], 60:40, v/v), ultrasonicated for 10 min, then shaken well and filtered (0.22 µm, nylon filtration). Continuous filtrate was determined by ultra-performance liquid chromatography (UPLC; general rule 0512, Vol. 4, Chinese Pharmacopoeia, 2015 Edition). Mobile phase A was 0.05% phosphoric acid solution and mobile phase B was acetonitrile; gradient elution was performed according to the procedures in Table 4. A Waters ACQUITY HSS T3 column (2.1 mm × 100 mm, 1.8 µm) was run at a flow rate of 0.5 ml/min in 40 °C. the injection temperature was 5 °C, and the detection wavelength was 210 nm. Each sample solution (1 µL) was precisely measured and injected into the liquid chromatograph while recording chromatograms. Samples containing only SOF or FOP were calculated according to the area normalization method; those containing SOF and FOP were calculated according to the area normalization method after removing the FOP peak area.

Table 4: Gradient process parameters for detection of related substances

Time (min)	Mobile phase A (%)	Mobile phase B (%)
Initial	98.5	1.5
3	98.5	1.5
19	58	42
25	58	42
30	20	80
30.5	98.5	1.5
36	98.5	1.5

3.3. Preparation of samples

3.3.1. Increasing the solubility of FOP

3.3.1.1. Disposal of FOP-API

FOP was micronized (FOP-micronized). FOP and lactose were mixed at ratios of 1:1 (m/m) and 1:2 (m/m). Then, the mixture (1:1) was micronized twice and the mixture (1:2) was micronized once. For the micronizing process, powders were micronized by fluid-energy mills; the pressure at the air outlet and intake were 0.6 MPa.

3.3.1.2. Contact angle measurement

Contact angles for samples described above and lactose (control) were measured using an integrated measurement and analysis system (DSA 30, Kruess Scientific Instruments, Germany). The contact angles, determined using drops of ultrapure distilled water, were measured at room temperature. The image of the water droplet was captured within 40 s of delivery. The contact angles of lactose were measured twice, while others were measured three times (Semprebon et al. 2017).

3.3.1.3. Determination of solubility

Solubility measurements of FOP were performed by adding a known excess amount of powders to 20 mL of 20 mmol acetate buffer solution (pH 4.0). Samples were agitated using a mechanical shaker at 50 rpm (37 °C ± 0.5 °C) for 4 h. The supernatants were filtered at 0.5, 1, 2, 3, and 4 h and analyzed by UPLC conditions

3.3.1.4. Scanning electron microscopy

Scanning electron microscopy (S-3400, Hitachi, Tokyo, Japan) was applied to observe the morphology of lactose and samples described in the 'Disposal of FOP-API' section. The samples were fixed using mutual conductive adhesive tape on aluminum stubs and sputter-coated with a gold layer at 20 mA for 30 s in an ion sputter coater (S-570, Hitachi, Tokyo, Japan) at a pressure of 8-10 Pa prior to the observation at an accelerating voltage of 5.0 kV.

3.3.2. Preparation of FOP/SOF FDCs

FOP (API, 18 g), SOF (API, 120 g), lactose (30 g), cross-linked carboxymethyl cellulose sodium (7.8 g), povidone (6 g), and microcrystalline cellulose (13.2 g) were weighed into a wet granulation pot for premixing for 600s (prepared for 300 pieces). Appropriate amounts of purified water were added to prepare soft materials, followed by filtering through a 32-mesh sieve. Preparations were dried to less than 2.0% moisture using a boiling dryer at 60±10 °C), then filtered through a 40-mesh sieve, thus yielding single granules. The dosage of magnesium stearate was calculated according to the particulate weight, then an 8.5 mm × 16 mm ellipsoid sheet was made with a tablet press, and the hardness was controlled between 80–110 N. Coating was conducted in a coating pot at 50±5 °C using coating solution 12% (m/m). The coating was stopped after the weight increased by 2–3%, and the samples were collected after drying.

3.4. *In vitro dissolution*

3.4.1. *In vitro dissolution*

The ChP paddle method (RC806D dissolution apparatus, Tianda Tianfa Technology Co. Ltd., Tianjin, China) was used for all the *in vitro* dissolution studies. In this method, 20 mmol acetate buffer solution (pH 4.0) containing 1% (w / v) sodium lauryl sulphate without enzyme, was used as dissolution media. The rate of stirring was 50±2 rpm. The amount of SOF/FOP was 400 / 60 mg in all formulations. The dosage forms were placed in 900 ml of dissolution media and maintained at 37±0.1 °C. At appropriate intervals (5, 10, 15, 20, 30, 45, 60, 90 and 120 min), 10 ml of the samples were taken and filtered through a 0.22 µm Millipore filter. The dissolution media was then replaced by 10 ml of fresh dissolution fluid to maintain a constant volume. After proper dilution, the samples were then analyzed by UPLC conditions. The mean of six determinations was used to calculate the drug release from each of the formulations.

3.4.2. *UPLC Conditions*

FOP reference (approximately 15 mg) and SOF reference (approximately 100 mg) were accurately weighed and diluted with 50% acetonitrile to give about 60 µg/mL FOP and 400 µg/mL SOF as the reference solution. One microliter each of reference substance and sample were taken and analyzed by UPLC (LC-30AD, Shimadzu Corporation, Japan) at wavelengths of 340 nm and 260 nm, respectively. Chrom-Core™ 120 C18 column (1.8 µm, 2.1 × 100 mm) was run at a flow rate of 0.4 ml/min at 40 °C Mobile phase A: 0.1% triethylamine in water (phosphoric acid, pH3.0 ± 0.1): acetonitrile (90:10); mobile phase B: acetonitrile. The analysis process was conducted according to the procedures in Table 5.

Table 5: Processes parameters of content detection method

Time (min)	Mobile phase A (%)	Mobile phase B (%)
Initial	100	0
8	100	0
9	50	50
10	50	50
11	100	0
12	100	0

3.5. *Pharmacokinetics studies*

Nine Sprague Dawley rats (male, 220-250 g), which were provided by the Shanghai SIPPR-BK Laboratory Animal Co. Ltd., were kept under standard laboratory conditions at a temperature of 25±2 °C and a relative humidity of 55±5 %. The rats were randomly divided into four groups: FOP tablets (Changzhou Yinsheng Pharmaceutical Co., Ltd), SOF tablets (Gilead), and FOP/SOF FDCs at a dose of 5.4 mg/kg of FOP and 36 mg/kg of SOF. The samples were ground into powder, which was dispersed in distilled water before administration. Blood samples (0.2 mL) were collected within 24 h from the jugular vein in heparinized tubes at 0.5, 1, 2, 3, 4, 6, 8, 14, 20 and 24 h after oral administration. The samples were centrifuged at 700 × g for 6 min immediately after collection, and the separated plasma was stored at -80 °C for analysis.

Table 6: Processes parameters of content detection of FOP

Time (min)	Mobile phase A (%)	Mobile phase B (%)
Initial	90	10
0.60	5	95
1.20	5	95
1.21	90	10
1.40	90	10

Plasma sample analysis: First, an aliquot of 40 µL of each plasma sample was protein precipitated with 400 µL methanol containing 100 ng/mL internal standard (IS; tolbutamide). The mixture was vortexed for 1 min and centrifuged at 18,000 ×g for 7 min. Two hundred microliters of supernatant were transferred to 96 well plates. An aliquot of 1 µL supernatant was injected for liquid chromatography-mass spectrometry (TQ5500 triple quad) analysis. Samples (20 µL) containing FOP were chromatographed on a reversed-phase Shim-pack GIST-FP C18-AQ column (3 µm, 2.1 × 50 mm). Mobile phase A: 0.1% formic acid in water; mobile phase B: 0.1% formic acid in acetonitrile. The analysis process was conducted according to the procedures in Table 6. The flow rate was 0.60 mL/min, and the oven temperature was 40 °C. The mass conditions were as follows: electrospray ionization (ESI-positive), multiple reaction monitoring (MRM) detection, FOP: Q1/Q3 masses, 780.30/554.40 Da, IS: Q1/Q3 masses, 271.10/172.00 Da. The concentration of FOP in each sample was calculated by reference to a calibration curve with a concentration range of 2-2000 ng/mL. The related pharmacokinetic parameters were analyzed using Phoenix WinNonlin 7.0.

Table 7: Processes parameters of content detection of FOP

Time (min)	Mobile phase A (%)	Mobile phase B (%)
Initial	95	5
0.10	95	5
0.60	10	90
1.10	10	90
1.11	95	5
1.40	95	5

Samples (20 µL) containing SOF were chromatographed on a reversed-phase CORTECS T3 column (2.7 µm, 2.1 × 100 mm). Mobile phase A: 0.1% formic acid in water; mobile phase B: 0.1% formic acid in acetonitrile. The analysis process was conducted according to the procedures in Table 7. The flow rate was 0.60 mL/min, and the oven temperature was 40 °C. The mass conditions were as follows: ESI (negative), MRM detection, PSI-6206 (a metabolite of SOF in plasma): Q1/Q3 masses, 259.10/238.90 Da, IS: Q1/Q3 masses, 269.20/106.10 Da. The concentration of PSI-6206 in each sample was calculated by reference to a calibration curve with a concentration range of 2–2000 ng/mL. The related pharmacokinetic parameters were analyzed using Phoenix WinNonlin 7.0 (Wang et al. 2020).

Acknowledgements: This study was supported by the National S&T Major Special Project on Major New Drug Innovations (2017ZX09201006-011& 2017ZX09201006-006). We thank Yuandong Biopharmaceutical Co., Ltd. Chengdu, Sichuan Province, China. for providing of instruments and venues and applying technical guidance and help.

Conflicts of interest: None declared.

References

Araujo A, Valenzuela-Granados V, Lopes AB, Michalczuk MT, Mantovani A, Alvares-da-Silva MR (2019) Sofosbuvir-based antiviral therapy in patients with recurrent HCV infection after liver transplant: A real-life experience. Ann Hepatol 18: 450–455.

Ascher DB, Wielens J, Nero TL, Doughty L, Morton CJ, Parker MW (2014) Potent hepatitis C inhibitors bind directly to NS5A and reduce its affinity for RNA. Sci Rep 4: 4765.

Aunins TR, Marsh KA, Subramanya G, Uprichard SL, Perelson AS, Chatterjee A (2018) Intracellular hepatitis c virus modeling predicts infection dynamics and viral protein mechanisms. J Virol 92: e02098–17.

Bangalore S, Kamalakkannan G, Parkar S, Messerli FH (2007) Fixed-dose combinations improve medication compliance: a meta-analysis. Am J Med 120: 713–719.

Bellesini M, Bianchin M, Corradi C, Donadini MP, Raschi E, Squizzato A (2020) Drug-drug interactions between direct oral anticoagulants and hepatitis c direct-acting antiviral agents: looking for evidence through a systematic review. Clin Drug Investig 40: 1001–1008.

Bhalerao H, Koteshwara KB, Chandran S (2020) Brinzolamide dimethyl sulfoxide in situ gelling ophthalmic solution: formulation optimisation and *in vitro* and *in vivo* evaluation. AAPS PharmSciTech 21: 69.

Cazzola M, Matera MG (2017) Fixed-dose combination inhalers. Handb Exp Pharmacol 237: 117–129.

Dietz J, Susser S, Vermehren J, Peiffer KH, Grammatikos G, Berger A, Ferenci P, Buti M, Mullhaupt B, Hunyady B, Hinrichsen H, Mauss S, Petersen J, Buggisch P, Felten G, Huppe D, Knecht G, Lutz T, Schott E, Berg C, Spengler U, von Hahn T, Berg T, Zeuzem S, Sarrazin C (2018) Patterns of resistance-associated substitutions in patients with chronic HCV infection following treatment with direct-acting antivirals. Gastroenterology 154: 976–988.

Dong W, Su X, Xu M, Hu M, Sun Y, Zhang P (2018) Preparation, characterization, and *in vitro*/*vivo* evaluation of polymer-assisting formulation of atorvastatin calcium based on solid dispersion technique. Asian J Pharm Sci 13: 546–554.

EMC (The electronic medicines compendium) The excipients of Sovaldi can be obtained from the website (2021): https://www.medicines.org.uk/emc/product/5247/smpc

Friedrich H, Fussnegger B, Kolter K, Bodmeier R (2006) Dissolution rate improvement of poorly water-soluble drugs obtained by adsorbing solutions of drugs in hydrophilic solvents onto high surface area carriers. Eur J Pharm Biopharm 62: 171–177.

Halfon P, Sarrazin C (2012) Future treatment of chronic hepatitis C with direct acting antivirals: is resistance important? Liver Int 32 Suppl 1: 79–87.
Heffernan A, Cooke GS, Nayagam S, Thursz M, Hallett TB (2019) Scaling up prevention and treatment towards the elimination of hepatitis C: a global mathematical model. Lancet 393: 1319–1329.
Heo YA, Deeks ED (2018) Sofosbuvir/velpatasvir/voxilaprevir: a review in chronic hepatitis C. Drugs 78: 577–587.
Iqbal B, Ali A, Ali J, Baboota S, Gupta S, Dang S, Shadab M, Sahni JK (2011) Recent advances and patents in solid dispersion technology. Recent Pat Drug Deliv Formul 5: 244–264.
Jantratid E, Janssen N, Reppas C, Dressman JB (2008) Dissolution media simulating conditions in the proximal human gastrointestinal tract: an update. Pharm Res 25: 1663–1676.
Lam AM, Espiritu C, Bansal S, Micolochick Steuer HM, Niu C, Zennou V, Keilman M, Zhu Y, Lan S, Otto MJ, Furman PA (2012) Genotype and subtype profiling of PSI-7977 as a nucleotide inhibitor of hepatitis C virus. Antimicrob Agents Chemother 56: 3359–3368.
Lam AM, Murakami E, Espiritu C, Steuer HM, Niu C, Keilman M, Bao H, Zennou V, Bourne N, Julander JG, Morrey JD, Smee DF, Frick DN, Heck JA, Wang P, Nagarathnam D, Ross BS, Sofia MJ, Otto MJ, Furman PA (2010) PSI-7851, a pronucleotide of beta-D-2'-deoxy-2'-fluoro-2'-C-methyluridine monophosphate, is a potent and pan-genotype inhibitor of hepatitis C virus replication. Antimicrob Agents Chemother 54: 3187–3196.
Leuner C, Dressman, J (2000) Improving drug solubility for oral delivery using solid dispersions. Eur J Pharm Biopharm 50: 47–60.
Li G, De Clercq E (2017) Current therapy for chronic hepatitis C: The role of direct-acting antivirals. Antiviral Res 142: 83–122.
Marks K, Naggie S (2019) Management of Hepatitis C in 2019. JAMA 322: 355–356.
McCown MF, Rajyaguru S, Le Pogam S, Ali S, Jiang WR, Kang H, Symons J, Cammack N, Najera I (2008) The hepatitis C virus replicon presents a higher barrier to resistance to nucleoside analogs than to nonnucleoside polymerase or protease inhibitors. Antimicrob Agents Chemother 52: 1604–1612.
Murakami E, Tolstykh T, Bao H, Niu C, Steuer HM, Bao D, Chang W, Espiritu C, Bansal S, Lam AM, Otto MJ, Sofia MJ, Furman PA (2010) Mechanism of activation of PSI-7851 and its diastereoisomer PSI-7977. J Biol Chem 285: 34337–34347.
NMPA CDE (Center for Drug Evaluation of National Medical Products Administration) The website for registration and information platform of clinical trial in China (2021) http://www.chinadrugtrials.org.cn/clinicaltrials.searchlist.dhtml.
Pan F, Chernew ME, Fendrick AM (2008) Impact of fixed-dose combination drugs on adherence to prescription medications. J Gen Intern Med 23: 611–614.
Sagnelli E, Starace M, Minichini C, Pisaturo M, Macera M, Sagnelli C, Coppola N (2018) Resistance detection and re-treatment options in hepatitis C virus-related chronic liver diseases after DAA-treatment failure. Infection 46: 761–783.
Sandmann L, Schulte B, Manns MP, Maasoumy B (2019) Treatment of chronic hepatitis C: efficacy, side effects and complications. Visc Med 35: 161–170.
Semprebon C, McHale G, Kusumaatmaja H (2017) Apparent contact angle and contact angle hysteresis on liquid infused surfaces. Soft Matter 13: 101–110.
Sofia MJ, Bao D, Chang W, Du J, Nagarathnam D, Rachakonda S, Reddy PG, Ross BS, Wang P, Zhang HR, Bansal S, Espiritu C, Keilman M, Lam AM, Steuer HM, Niu C, Otto MJ, Furman PA (2010) Discovery of a beta-d-2'-deoxy-2'-alpha-fluoro-2'-beta-C-methyluridine nucleotide prodrug (PSI-7977) for the treatment of hepatitis C virus. J Med Chem 53: 7202–7218.
Tao X, Wang N, Wang J, Fu Z, Gu Z, Zhang Y, Chen S, Wang L, Yu L (2019) Preclinical evaluation of Amphihevir, a first-in-class clinical Hepatitis C virus NS4B inhibitor. Antimicrob Agents Chemother 63: e01237–19.
Torre LA, Siegel RL, Ward EM, Jemal A (2016) Global cancer incidence and mortality rates and trends--an update. Cancer Epidemiol Biomarkers Prev 25: 16–27.
Villani R, Vendemiale G, Serviddio G (2019) Molecular mechanisms involved in HCC recurrence after direct-acting antiviral therapy. Int J Mol Sci 20: 49.
von Felden J, Vermehren J, Ingiliz P, Mauss S, Lutz T, Simon KG, Busch HW, Baumgarten A, Schewe K, Hueppe D, Boesecke C, Rockstroh JK, Daeumer M, Luebke N, Timm J, Schulze Zur Wiesch J, Sarrazin C, Christensen S (2018) High efficacy of sofosbuvir/velpatasvir and impact of baseline resistance-associated substitutions in hepatitis C genotype 3 infection. Aliment Pharmacol Ther 47: 1288–1295.
Wang NY, Zuo WQ, Xu Y, Gao C, Zeng XX, Zhang LD, You XY, Peng CT, Shen Y, Yang SY, Wei YQ, Yu LT (2014) Discovery and structure-activity relationships study of novel thieno [2,3-b] pyridine analogues as hepatitis C virus inhibitors. Bioorg Med Chem Lett 24: 1581–1588.
Wang J, Yang L, Li D, Xu Y, Yang L, Zhao H, Zhu Z, Luan H, Luo Q (2019) Investigating the mechanism of l-valine in improving the stability of gabapentin combining chemical analysis experiments with computational pharmacy. AAPS PharmSciTech 20: 114.
Wang T, Babusis D, Park Y, Niu C, Kim C, Zhao X, Lu B, Ma B, Muench RC, Sperger D, Ray AS, Murakami E (2020) Species differences in liver accumulation and metabolism of nucleotide prodrug sofosbuvir. Drug Metab Pharmacokinet 35: 334–340.
WHO (World Health Organization) Global hepatitis report, 2017 (2017). Available from: https://www.who.int/hiv/pub/hepatitis/global-hepatitis-report2017-executive-summary/zh/